ISSN : 0974 - 7494 Volume 7 Issue 3

Trade Science Inc.

Nano Science and Nano Technology
An Indian Journal

Full Paper

NSNTAIJ, 7(3), 2013 [108-113]

Morphology and optoelectrical properties study of nano/micro structures silicon layer prepared by photo electrochemical and electrochemical etching

Nadir F.Habubi[1]*, Raid A.Ismail[2], Hasan A.Hadi[3]

[1]Dep. Physics-Education faculty-The University of Mustanseriyah-Baghdad, (IRAQ)

[2]Dep. of Applied Sciences-The University of Technology – Baghdad, (IRAQ)

[3]Dep. Physics-Education faculty-The University of Mustanseriyah-Baghdad, (IRAQ)

E-mail : nadirfadhil@yahoo.com, hadihasan@hotmail.co.uk, raidismail@yahoo.com

ABSTRACT

In this work, Electrochemical Etching, (ECE) and Photo Electrochemical Etching, (PECE) were used to produce porous silicon for p-type and n-type (111) orientation. The Root-mean-square (RMS) surface roughness is a commonly accepted parameter to describe surface by imaging techniques Atomic Force Microscopic (AFM) was used to analyse the surface sample. The effect of type substrate on a surface porous morphology by optical microscope have been examined. the dependence of porous silicon morphology on fabrication conditions and the link between morphology, photocurrent, and energy gap of porous silicon layer (PS)have been determined.

INTRODUCTION

Porous silicon (PS) has many unique characteristics such as direct and wide modulated energy band gap, high resistivity, vast surface area-to-volume ratio and the same single-crystal structure as bulk. Physical features of porous silicon are connected with quantum confinement effects, i. e., with a change of the band diagram and increase of effective band gap. Distinction in absorption of the light by PS and crystalline silicon is that in PS the pores can play a role of waveguides. The light got in a pore, after repeated reflections from the pore walls will penetrate far deep into PS. At the expense of it, PS absorbs light more strongly than bulk silicon. Therefore, it is promising for creation of photodetectors on the PS base. These advantages make it a suitable material for photodetectors[1]. Silicon nanocrystal have been shown to possess intriguing properties, such as band gap control with nanocrystal size, very fast optical transition, and multiple carrier generation[2].

EXPERIMENTAL DETAILS

Electrochemical etching

The silicon wafer serves as the anode. The cathode is made of platinum or any HF-resistant and conducting material. The cell body itself is, in general, made of highly acid-resistant polymer such as Teflon. Since the entire silicon wafer serves as the anode, PS is formed on any wafer surface in contact with the HF solution, including the cleaved edges. Figure 1 shows a schematic design of PS system.

Photo electrochemical etching

As shown in Figure 2, in this case by illuminating n-type substrates, surface of the wafer with sufficiently energetic photons, holes can be photo-generated in the bulk. Illuminating n-type substrates surface by the di-

ode laser (red-650nm) and power of 30mW To get etched area≅ $1cm^2$, a double-concave lens is used.

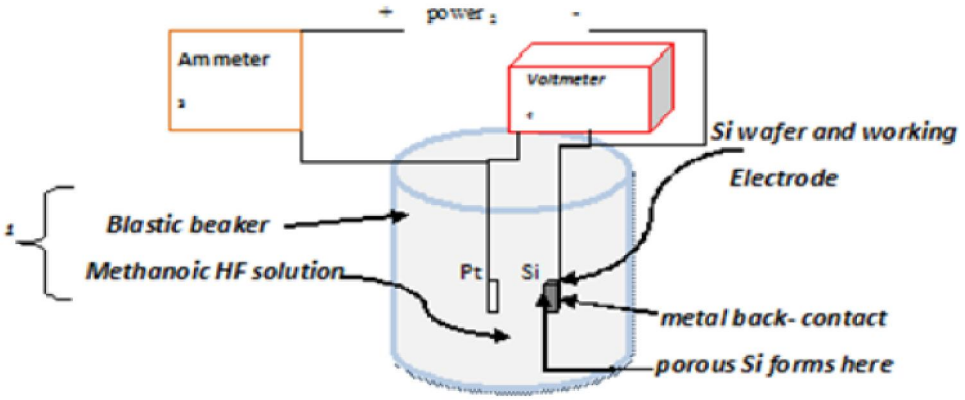

Figure 1 : Schematic diagram for the designed porous silicon fabrication system.

Sample preparation

The experiments, Porous silicon films were produced using monocrystalline silicon wafers p and n-type, with resistivity's (14-22) Ω.cm, and 10 Ω.cm respectively having a (111) orientation. Samples were made of porous silicon produced with a standard technique of anodizing p and n-Si silicon substrates in an electrolyte HF (40%) :(99.8) % CH_2OH (with a 1:1 volume ratio) under constant etching current density of 60 mA/cm² at 10min etching time. Methanol and alcohol are used commonly to clean the wafer by immersing it in these chemicals in turn, in the ultrasonic bath for few second. The average porous layer thickness and the porosity were measured by gravimetric methods. The samples were thermally oxides in air (at 300 °C for 30 min). top Al/PS/c-Si/bottom Al was shown in Figure 3. To ensure an uniform current distribution as possible, the samples were coated with ≈800 nm layer of aluminum on the backside. The evaporation was performed in a vacuum pressure of 10^{-6} torr, using an evaporation plant model "E306 A manufactured by Edwards high vacuum". In this work, an AA 3000 Scanning Probe Microscope AFM system in School of applied sciences, University of Technology has been used. The current passing through the device was measured using a UNI-T UT61E Digital Multimeters. This measurements was done under light of different illumination power densities supplied by a Halogen lamp 150W which is connected to a variac and calibrated by a power-meter. The photosensitivity of the photodetector was investigated in the wavelength range of 400-1000 nm with the aid of Joban-Yvon monochromatic and standard Si power-meter.

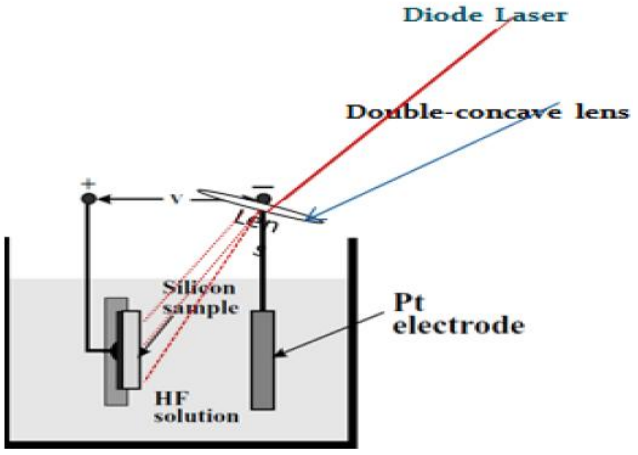

Figure 2 : Schematic diagram of the porous silicon fabrication system.

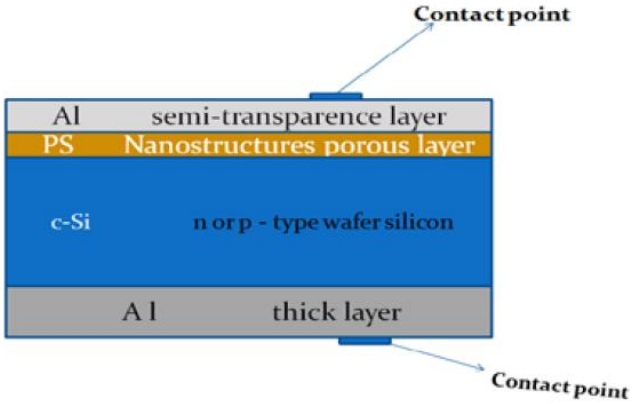

Figure 3 : Cross-sectional view Al/PS/c-Si/Al sandwich structure.

RESULTS AND DISCUSSION

X-ray diffraction

Figures 4 and 5 show the X-ray diffraction patterns of the porous structure on p-Si and n-Si substrate

Full Paper

at different etching current density respectively. A peak becomes very broad with varying full-width at half maximum as shown in Figures 4-5 which confirm the formation of porous structure on the crystalline silicon surface at 40 mA/cm^2. At high etching current density large than 60mA/cm^2 XRD spectra showed that the structure is amorphous.

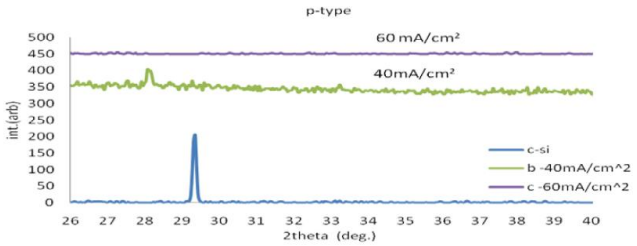

Figure 4 : XRD spectra of c-Si and PS samples anodized for 10 min at b) 40mA.cm^{-2}, and c) 60mA.cm^{-2}.

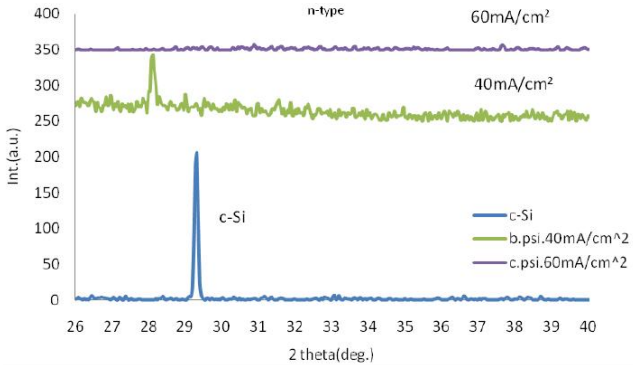

Figure 5 : XRD spectra of c-Si and PS samples anodized for 10 min at b) 40mA.cm^{-2}, and c) 60 mA.cm^{-2}.

According to the theory of propulsion the essential tensile stresses are produced both in porous silicon and in Si substrates. Therefore, the micro cracks are formed in PS and that serve as easy path for further pore growth[9].

SEM

The structural properties of PSi layer such as surface morphology, specific surface area, pore width, pore shape, thickness of walls between pores, and layer thickness have been studied in this work by using SEM. Figure 6 shows the electron micrograph of inclined silicon surface etched with 40mA/cm^2. This figure confirms formation of columnar grains arranged periodically along the etched surface.

AFM

Two and Three-dimensional AFM image of the as-anodized porous silicon surface structure formed on n- and p- type for 10 min etching time 60 mA/cm^2 etching current density are shown in the following figures. The PS layer thickness and roughness are not monotonically proportional to the anodization time. The surface morphology measured by AFM is given in Figures 7 and 8, which show that the surface of the PS layer consists of inhomogeneous and large number of irregularly shaped distributed randomly over the entire surface. Representative 5 µm x 5 µm images two and three dimension of porous silicon with various etching time are shown in Figures 7 and 8. The surface of the etched PS layer consists of a matrix of randomly distributed nanocrystalline Si pillars which have the same direction and AFM images also show voids that the uniformity. Root-mean-square (RMS) surface roughness is a commonly accepted parameter to describe surface. It is typically used to quantify variations in surface elevation, the RMS roughness for p-type is found to be 24 nm and n-type was 5.52 nm; also the Sz.(Ten Point height) was 50.9 nm for n-type and 199 nm for p-type, With large irregular upright structure of silicon crystallites. It is clear that the formation porous layer depends on the substrate type. The change of these values in RMS for n and p-type agree with Hong and Lee[4]. These different morphologies are the result of different pore formation mechanisms. Many mechanisms are thought to contribute to the electrochemical pore growth process in silicon, and the morphology resulting from a given experiment is usually determined by a combination of several of these[5].

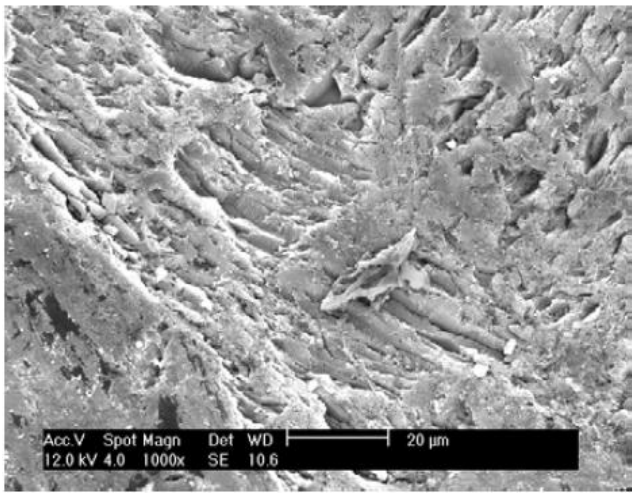

Figure 6 : SEM micrograph of PS prepared with J=40 mA/cm^2.

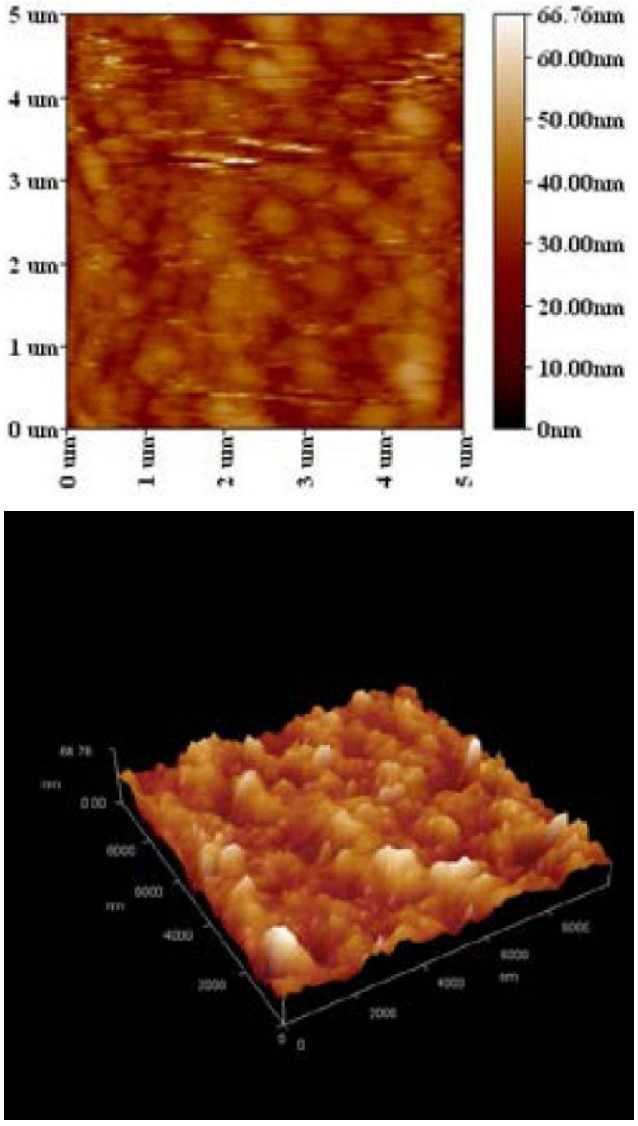

Figure 7 : 2D and 3D AFM images of PS surface at constant current density 60mA/cm^{-2} and at 10min etching time for n-type (5µm×5µm).

Optical microscopy

From Figure 9, optical micrograph shows that the distinct variation between the fresh silicon surface and the porous silicon surfaces formed at 40mA/cm^2 etching current density for 10 min etching time. The sample exhibited high density of small pores distributed over the etched region where there is big difference between the non-etched and etched silicon surfaces as shown in Figures 6 and 7. The porous surface shows different colors as shown in Figure 7; also some time close to red resulting may be sub oxide of silicon. This confirms the anodic dissolution of the silicon surface leading to porous structure formation and the visual observation of the silicon surface is considered as a very important feature gave photoluminescence.

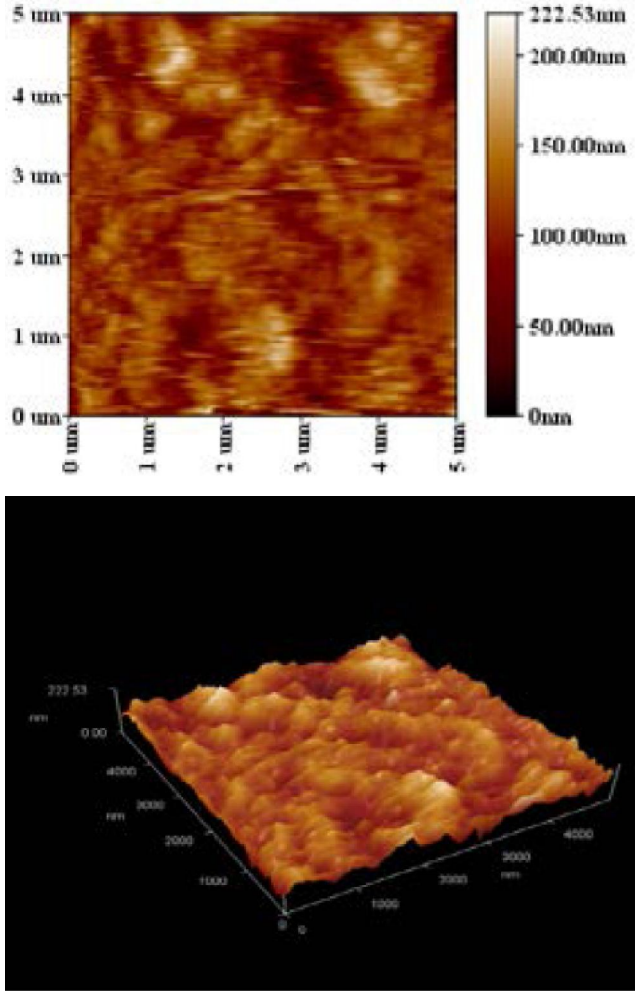

Figure 8 : 2D and 3D AFM images of PS surface at constant current density 60mA/cm^{-2} and at 10min etching time for p-type (5µm×5µm).

Photoluminescence in simple terms is a reverse process of absorption, so the different color resulting from broadening of the band gap energy occurs when there is a decrease in the crystallite size. (PL) at room temperature when compared to a fresh c-Si surface for p-Si and n-Si.

Illuminated current –voltage

Figures 10 and 11 show the reversed current-voltage characteristics of the device measured in dark and under different light intensity illumination, the photocurrent under a (1.2-20) mW/cm^2 tungsten lamp illumination, also this figure explains the J-V characteristics sandwiches Al/PS/p-Si/Al and Al/PS/n-Si/Al structure under illumination with constant etching time. It can be

Full Paper

seen that the reverse current value at a given voltage for the Al/PS/c-Si/Al heterojunction under illumination is higher than that in the dark. It increases with the increase of light intensity. Increasing the bias voltage increases the photocurrent. The photocurrent decreases with increasing preparation current density, etching time, etc. The increasing value of resistivity is due to increasing the PS layer thickness, but as shown in the figures, there are increase in photocurrent at increasing PS layer thickness in p-type. This may due to the excessive etching process which leads to increase of porosity of the porous silicon layer and hence improve the sensitivity of the formed junction between the crystalline silicon and the PS layer[3]. Figure 12 demonstrates the dependence of photocurrent on light power density. It is clear that the relationship is linear and the Al/PS/p-Si/Al photodetector has good linearity characteristics compare with the Al/PS/n-Si/Al photodetector.

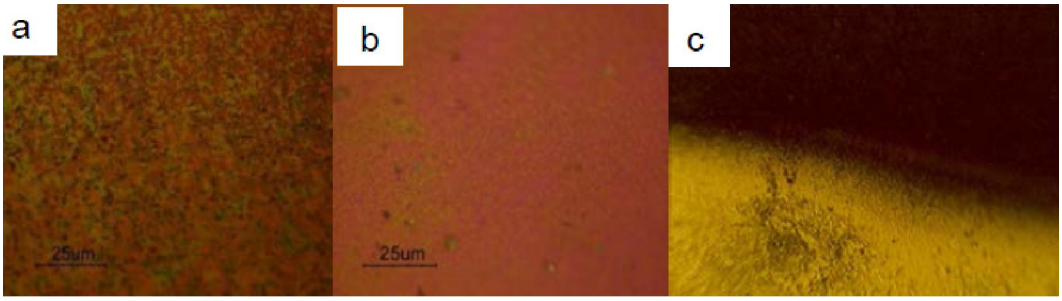

Figure 9 : [a] and [b] optical micrograph of PS surface on p-Si and n-Si formed at 60mA/cm2 etching current density for 10min etching time; [c] Optical images of cross-sections of porous silicon PS/Si –interface.

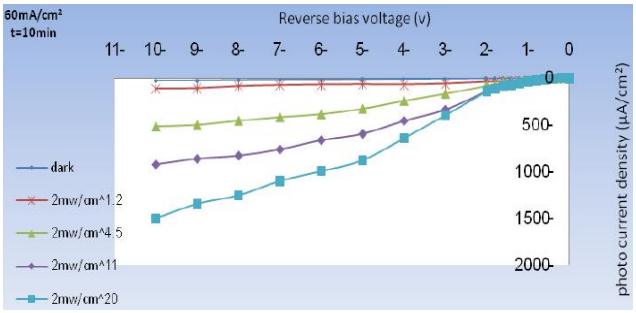

Figure 10 : Photocurrent of PS/p-Si heterojunction as a function of reverse bias illuminated for different power density at 10 min etching time, 60mA/cm^2.

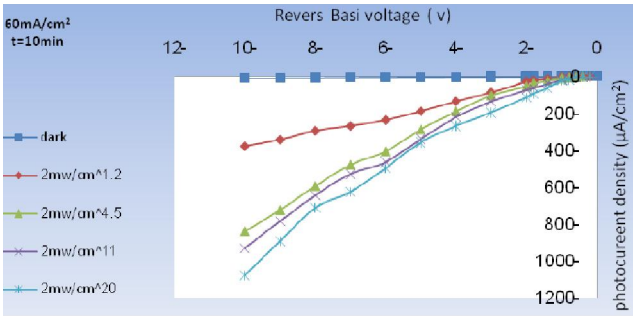

Figure 11 : Photocurrent of PS/n-Si heterojunction as a function of reverse bias illuminated for different power density at 10 min etching time 60mA/cm^2.

Energy gap of porous silicon

The value of energy gap is determined by the photoresponse spectrum curve between photocurrent and energy of quanta of the incident light. In the case of nano- or micro-porous silicon, quantum confinement causes spatial fluctuations of the effective band gap as can be seen in Figures 13 and 14 for p-type and n-type, so as[6,7] reported that the porous layer behaves as wide band semiconductor sensitive to the visible light. Figures 13 and 14 show the energy gap for the investigated sample is large than 1.1eV, and for nanostructure PS layer was 2.26eV, while it was 1.9eV for microstructure PS layer. The enhancing of band gap in PS is related to quantum-size effect. The main quantum confinement effect is represented by the appearance of new energy levels in the silicon band gap. The increased band gap resulting from quantum - confinement excludes valence band holes from these smallest regions of the porous silicon matrix[8].

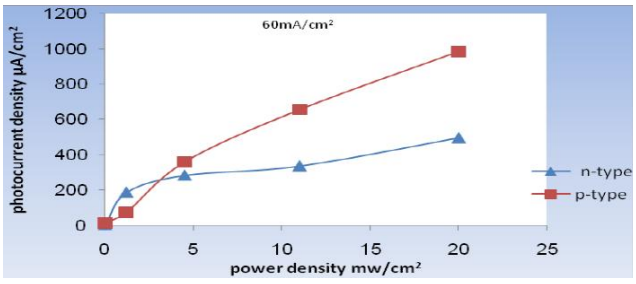

Figure 12 : Photocurrent density of PS/p-Si and PS/n-Si heterojunction as a function power density for different etching time at 5v reverse bias.

CONCLUSION

The dimensions and morphology of the pores can be controlled by anodization parameters. Porous silicon was anodized on n-type silicon with laser light and on p-type silicon in dark, using a current density of 60 mA/cm^2 etching current density for 10 min etching time. We demonstrated that it is possible to use the AFM to obtain information of the surface of porous layers, such as surface roughness and thickness. The Al/PS/n-Si/Al photodetector has the performance of photocurrent ~ 1079μA under 20 mW/m^2 illuminations and dark current ~ 0.08μA, while the Al/PS/p-Si/Al photodetector has the performance of photocurrent ~ 1500μA and dark current ~ 26 μA at the same condition. The low-energy gap at 1.9 eV was obtained in PS with characterized by the thickness 222.53 nm for p-type and the high-energy gap at 2.26 eV was obtained in PS with characterized by the thickness 66.76 nm for n-type. The peak shifts towards the higher energy side, which supports the quantum confinement effect in porous silicon.

REFERENCES

[1] K.Lee, Y.Tseng, C.Chu; Ahigh-gain porous silicon metal–semiconductor–metal photodetector through rapid thermal oxidation and rapid thermal annealing, Appl.Phys.A, **67** 541–543 **(1998)**.

[2] Sang-Kyun Kim, Baek-Hyun Kim, Chang-Hee Cho, Seong-Ju Parka; Size-dependent photocurrent of photodetectors with silicon nanocrystals, Applied Physics Letters, **94**, 183106 **(2009)**.

[3] A.M.Alwan, A.A.Jabbar; Design and fabrication of nanostructures silicon photodiode, Modern Applied Science, **5(1)**, 106-112 **(2011)**.

[4] K.Hong, C.Lee; The Structure and optical properties of n-type and p-type porous silicon, Journal of the Korean Physical Society, **42**, S671-S675, February **(2003)**.

[5] X.G.Zhang; Morphology and formation mechanisms of porous silicon, J.Electrochem.Soc., **151(1)**, C69–C80 **(2004)**.

[6] D.F.Timokhov, F.P.Timokhov; Semiconductor Physics, Quantum & Optoelectronics, **6(3)**, 307-310 **(2003)**.

[7] D.F.Timokhov, F.P.Timokhov; Determination of structure parameters of silicon by the photoelectric method, Journal of Physical Studies, **8(2)**, 173-177 **(2004)**.

[8] Michael; Porous silicon in practice: Preparation, characterization and applications, 1st Edition, Published 2012 by Wiley-VCH Verlag GmbH & Co. KGaA, 15 **(2012)**.

[9] V.Parkhutik; Porous silicon–mechanism of growth and applications, Solid-state Electron, **43**, 1121-1141 **(1999)**.